

Optimization of Hot Forging Process Using CAE Simulation and RSM Method

Nguyen Thi Thanh Mai¹, Tran Cong Minh¹, Phan Nhu Ngoc¹, Le Thi Phuong¹, Nguyen Van Luong¹, Hoang Hai Phong^{1*}

¹School of Mechanical and Automotive Engineering, Hanoi University of Industry, Vietnam, 0100000
Corresponding Author: hoanghaiphong@hau.edu.vn

Abstract— Forging is one of the methods of manufacturing turbine blades. However, due to the complexity of the knife style, they cannot be produced in one step and use is required. In this paper, the extruded elliptical cross-section is considered as the skirt, followed by the response surface. Use CAE and this optimization RSM method. NX software is used for design. In addition, Qform software is also used to simulate the attack process. The optimized sample is compared with the sample generated from the conventional design method. The results show that the optimal chemical method gives better results than the conventional method.

Keywords— QForm, Hot forging, FE Simulation, Stainless Steel Forging, Turbin blade Forging, RSM.

I. INTRODUCTION

Hot forging is a method of processing metal under pressure in a hot state, widely used in processing motorbike engines [1] and gears [3] thanks to its outstanding advantages such as less waste. Material, more durable than other types. method. The design process of hot stamping dies in S20C steel is based on stamping standards and instructions such as GOST 7075-89; IN EN 10243-1; DIN EN 10243-2;... First, when designing a stamping die for each type of mold, it is necessary to look up and determine the parameters according to the standards recorded in documents and forging handbooks. Then, based on those parameters, proceed to fabricate the forging mold. Finally, after the mold is completely manufactured, detailed forging and quality assessment are carried out, confirming defects, finding the cause and then repairing the mold or workpiece shape. Until the finished product satisfies the established technical requirements, this process is repeated. One benefit of this design method is that the final product satisfies technical requirements, and the design process is transparent and straightforward. But this approach also has a number of noteworthy drawbacks. Before being used in the real production process, the mold set must first be evaluated and then repeatedly altered. Secondly, it can take a lot of testing to finish a mold set. This translates into lost testing time, wasted workpiece material, higher manufacturing costs, and worse economics. These factors make simulation software, which minimizes design time and improves product economics, the most accurate option for improving mold and blank designs [4].

To overcome the above shortcomings and difficulties when forging parts made from S20C material, the article presents an evaluation of the optimal method for the production process of S20C Figure 1 fan blades by simulation. Finite element (FE) simulation allows finding a suitable mold design and optimal workpiece shape. Simulation also generates die profile geometry to compensate for elastic deformation of the die and produce geometric accuracy of the stamped product. Plastic cracks in stamping materials can be predicted and minimized

by simulation [5]. The presented model is realized in the metal forming simulation software QForm 10. The software automatically applies theory to the analysis process, including plastic deformation methods and finite element modeling. is depicted in Figure 2. The results of this work help predict loops, identify incomplete defects, and pressures required for the actual process. From there, find the most optimal forging blank.

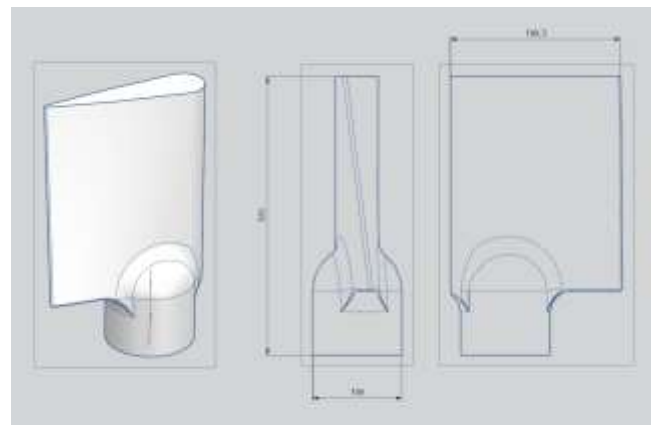


Figure 1: Finished product model

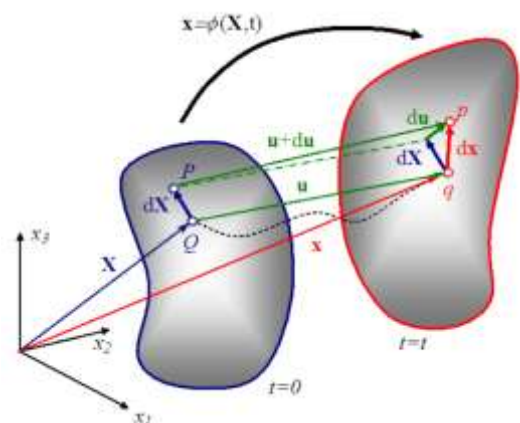


Figure 2. Description of geometric plastic deformation

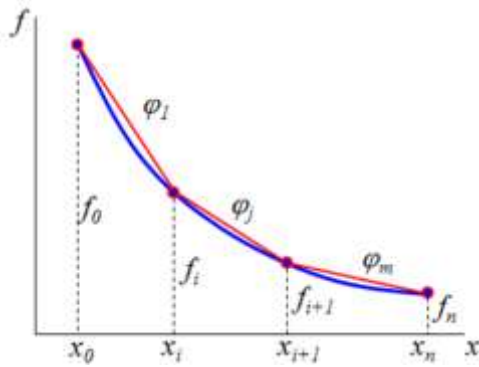


Figure 3. Diagram depicting the finite element method

The applied formula of the finite element method:

$$f(x) = \sum_{m=1}^M \varphi_m(x); \varphi_m(x) = \frac{f_{n+1} - f_n}{x_{n+1} - x_n} (x - x_n)$$

In addition, there are a number of other related scientific theories such as friction force during plastic deformation, metal flow pressure,...

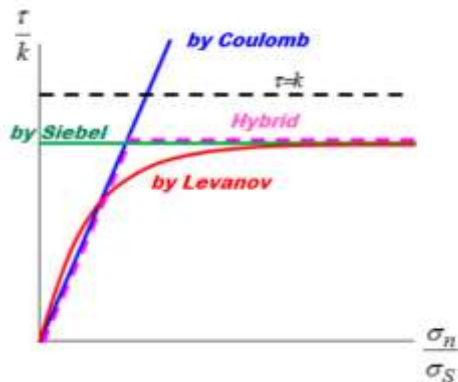


Figure 4. Diagram of the intersection between friction theories.

II. INITIAL EMPLOYMENT DESIGN METHOD

The initial blank was designed for two separate parts of the blade: the airfoil and the root. A circular cross-section is considered for the root section of the final blade of the same diameter, and an elliptical cross-section is chosen for the airfoil section. Previous investigations have shown that elliptical extrusion forging allows better material flow, uniformly distributed plastic deformation and relatively low contact pressure and is more cost-effective than forming operations. before (Ou and Balendra 1998). Finally, as shown in Fig. 5, for optimization purposes, root length (L1), full length of blade (Lt), large elliptical airfoil diameter (D1), the small diameter elliptical airfoil (D2) and the radius of the root and airfoil joint (R) are selected as optimization parameters. In the RSM method, the minimum and maximum values of the parameters must be entered as input to the software. The minimum dimensions of the workpiece were chosen to yield a workpiece volume equal to the final part, and the maximum size of the workpiece was chosen to yield a workpiece volume 1.6 times larger than the last part. Minimum and maximum values are shown in Table 1

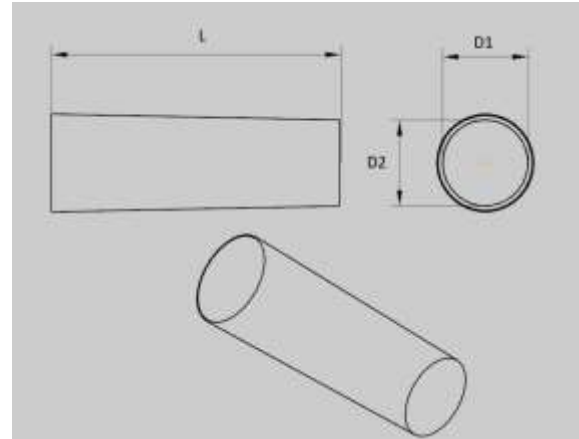


Figure 5: Initial design workpiece model

TABLE 1. Maximum and smallest dimensions of the initial embryo

| Dimension | Min value (mm) | Giá trị lớn nhất (mm) |
|----------------|----------------|-----------------------|
| L | 315 | 325 |
| D ₁ | 95 | 105 |
| D ₂ | 95 | 105 |

III. SIMULATION IN QFORM

The hot forging process is simulated using Qform 10. It is necessary to determine the degree of filling, temperature, stress, and degree of deformation of the workpiece. Parameters such as stress and strain levels achieve accurate results through the simulation process.

S20C: "S" usually represents "Steel" and "20C" is the proportion of carbon in the steel composition.

During the hot stamping process, S20C steel can be used to produce a variety of products, from machine parts to precision mechanical parts.

The properties of hot stamping products from S20C steel depend on the specific production process, including heating temperature, stamping pressure, and cooling process after stamping. For specific applications, additional processing processes such as machining or applying protective coatings may be required to meet specific shape, size, and property requirements.

TABLE 2. Chemical composition of C45 steel.

| Steel grade | Chemical Composition % | | | | | | |
|-------------|------------------------|------|---------|-------|-----|-----|-----|
| | C | Si ≤ | Mn | P ≤ | Cr | Ni | Mo |
| S20C | 0,17÷0,24 | 0,4 | 0,4÷0,7 | 0,045 | 0,4 | 0,4 | 0,1 |

TABLE 3. Forging process parameters

| Raw-Forging | |
|---------------------------------|--------------------------|
| Workpiece material | S20C |
| Workpiece temperature | 1200°C |
| The material | SKD62 |
| Workpiece temperature | 600° |
| Machine | Mechanical Press C86-150 |
| Lubrication | Graphite + water |
| Stop condition: Tool 2 to tool1 | 0 mm |

Mold filling is considered one of the goals of optimization, although it must be quantified to apply in data. Below we have the simulation results shown in Table 4.

TABLE 4. Design simulation results

| Std | Run | D1 | D2 | L | Mean stress (Mpa) | Load (MN) |
|-----|-----|-----|-----|-----|-------------------|-----------|
| 1 | 1 | 95 | 95 | 320 | -342.4 | 60.4 |
| 4 | 2 | 105 | 105 | 320 | -746.8 | 70.6 |
| 7 | 3 | 95 | 100 | 325 | -770 | 78.7 |
| 3 | 4 | 95 | 105 | 320 | -578 | 71.7 |
| 12 | 5 | 100 | 105 | 325 | -832.6 | 95.9 |
| 2 | 6 | 105 | 95 | 320 | -572.4 | 70.2 |
| 14 | 7 | 100 | 100 | 320 | -664.3 | 70.9 |
| 15 | 8 | 100 | 100 | 320 | -659.6 | 70.4 |
| 8 | 9 | 105 | 100 | 325 | -832.6 | 96.1 |
| 11 | 10 | 100 | 95 | 325 | -763.8 | 78.3 |
| 9 | 11 | 100 | 95 | 315 | -286.1 | 41.83 |
| 5 | 12 | 95 | 100 | 315 | -281.5 | 39.83 |
| 13 | 13 | 100 | 100 | 320 | -670.9 | 75.1 |
| 10 | 14 | 100 | 105 | 315 | -771.1 | 92.9 |
| 6 | 15 | 105 | 100 | 315 | -794.8 | 91.1 |

IV. RESPONSE SURFACE METHOD

Response surface methodology (RSM) is an effective method for solving multivariate and objective optimization problems. Experimental groups are designed using reasonable experimental design methods, and some reliable data can be obtained through testing or simulation. To accommodate the functional relationship between various factors and response values, multiple quadratic regression equations are used. By analyzing the regression equations, the best parameter combination is determined. This method is widely used in the field of metal forming because of its small computational characteristics, interaction between analytical factors and high convergence.

In this study, the survey simulation results show that with D1=90÷105; D2=90÷105 and L=315÷325, the cavity is completely filled, the product meets technical requirements. To optimize the workpiece size, while achieving the goal of minimum Mean stress and minimum maximum stamping force, the multi-objective optimization method uses RSM (Response Surface Methodology), with ma The Box-Behnken experimental match is used.

Building an empirical matrix: Using the Box-Behnken empirical matrix, with the number of variables being 3, we have an empirical matrix consisting of 15 experiments as shown in table 4:

Analysis results with Mean Stress (Y1):

| Source | Sum of Squares | df | Mean Square | F-value | p-value | significant |
|-------------|----------------|----|-------------|---------|---------|-------------|
| Model | 4.709E+05 | 5 | 94173.67 | 20.82 | 0.0001 | significant |
| A-D1 | 1.188E+05 | 1 | 1.188E+05 | 26.26 | 0.0006 | |
| B-D2 | 1.161E+05 | 1 | 1.161E+05 | 25.67 | 0.0007 | |
| C-L | 1.419E+05 | 1 | 1.419E+05 | 31.38 | 0.0003 | |
| AC | 50782.62 | 1 | 50782.62 | 11.23 | 0.0085 | |
| BC | 43305.61 | 1 | 43305.61 | 9.57 | 0.0128 | |
| Residual | 40707.52 | 9 | 4523.06 | | | |
| Lack of Fit | 40643.07 | 7 | 5806.15 | 180.18 | 0.0055 | significant |
| Pure Error | 64.45 | 2 | 32.22 | | | |
| Cor Total | 5.116E+05 | 14 | | | | |

Figure 6: ANOVA analysis results for Mean Stress Y1.

The analysis results show that the p-value for Model, D1, D2, L are all very small compared to the significance level of 0.05, meaning that the influence of all input parameters on Mean Stress is large.

Regression model for Mean Stress (Y1):

$$Y1 = -637.79 - 121.84 * D1 - 120.47 * D2 - 133.19 * L + 112.67 * D1 * L + 104.05 * D2 * L$$

In this regression model, R2=0.9204 and adjusted R2=0.8762 show that the regression model is appropriate.

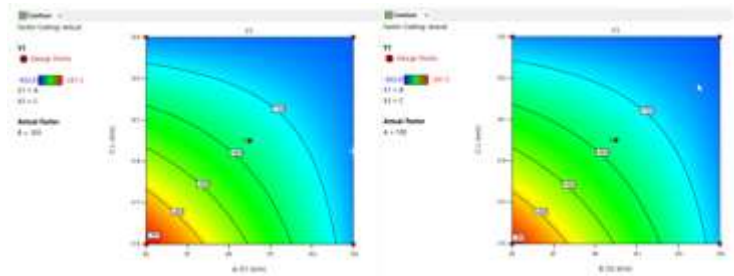


Figure 7: Contour plot for Mean Stress with D1, D2 and L.

ANOVA analysis for Max load Y2:

| Source | Sum of Squares | df | Mean Square | F-value | p-value | significant |
|-------------|----------------|----|-------------|---------|---------|-------------|
| Model | 2423.88 | 3 | 807.96 | 4.83 | 0.0249 | significant |
| A-D1 | 748.26 | 1 | 748.26 | 4.48 | 0.0605 | |
| B-D2 | 807.42 | 1 | 807.42 | 4.83 | 0.0527 | |
| C-L | 868.19 | 1 | 868.19 | 5.19 | 0.0459 | |
| Residual | 1672.02 | 10 | 167.20 | | | |
| Lack of Fit | 1671.90 | 9 | 185.77 | 1486.13 | 0.0201 | significant |
| Pure Error | 0.1250 | 1 | 0.1250 | | | |
| Cor Total | 4095.90 | 13 | | | | |

Figure 8: ANOVA analysis for Max load Y2.

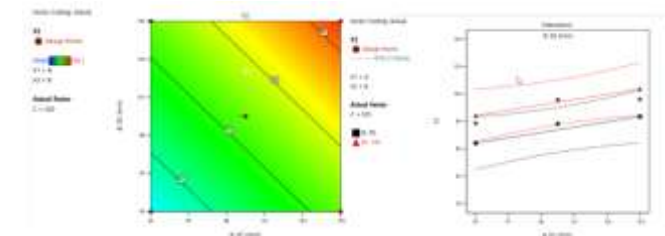


Figure 9: Contour plot for Max Load with D1, D2 and L.

The overall model has an F value of 4.83 and a p value of 0.0249, indicating that this model is statistically significant at the 5% significance level. This means that the model is capable of explaining a portion of the variation in the data. Among the factors, only the C-L factor is statistically significant, with a p value of 0.0459, less than the 5% significance level.

The analysis results show that the p-values of D1 and D2 are both greater than the significance level of 0.05. p-value of L=0.0459, less than 0.05. Predicted R² of 0.1175 is not as close to Adjusted R² of 0.4693 as expected; meaning the difference is greater than 0.2. This may indicate a large mass effect or there may be a problem with your model and/or data. Factors to consider include model reduction, response variability, outliers, and more. All empirical models should be tested by performing validation runs. Adeq Precision measures signal-to-noise ratio. A ratio greater than 4 is desirable. Your ratio of 5.921 shows sufficient signal. This model can be used to navigate the design space.

Difference between Predicted R² and Adjusted R²: Predicted R² (0.1175) is much lower than Adjusted R² (0.4693), with a difference greater than 0.2. This suggests that the model's ability to predict new data is much weaker than its ability to fit existing data. Large differences can indicate a number of problems such as: large mass effects, the model may be overfit or not properly specified, or the data may have quality issues such as outliers or Inaccurate measurement.

From the ANOVA analysis, the regression model of Mean Stress is:

$$Y2=73.49+9.67*D1+10.05*D2+10.42*L$$

Although Adjusted R² is quite high (0.4693), Predicted R² is very low (0.1175), showing that the model's predictive ability is weak. A large difference between Predicted R² and Adjusted R² (> 0.2) suggests that the model may be experiencing mass effect problems or have modeling errors.

V. OPTIMIZATION

Multi-objective optimization problem:

Find $Y=f(D1, D2, L)$ so that Y1 is the smallest and Y2 is the smallest

(Y1: Mean Stress; Y2: maximum load)

Using the Desirability Function Approach with existing experimental results, based on the lateral conditions of the multi-objective optimization problem (Figure 10), we have the optimization results as Figure 11:

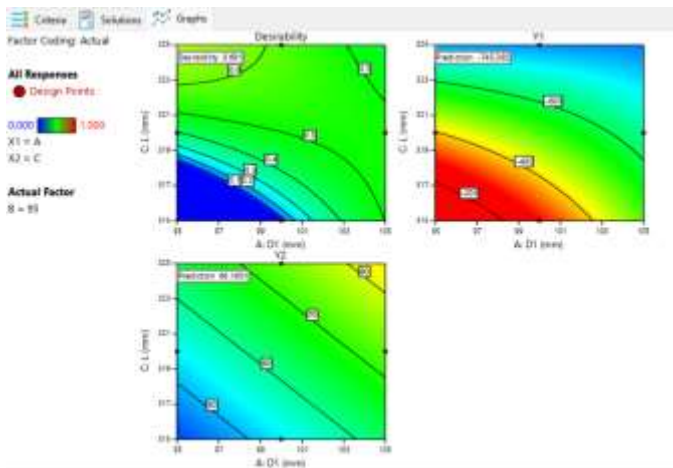


Figure 10: Desirability graph of elements A (D1), B (D2), C (L)

The graph Figure 10 shows the relationship between Desirability and three factors A (D1), B (D2), and C (L), as

well as the influence of these factors on Y1 (Mean Stress responses.) and Y2 (Max Load).

Desirability vs A, B, C:

- As A (D1) increases from 95 to 105, Desirability decreases.
- As B (D2) increases from 95 to 105, Desirability decreases.
- When C (L) increases from 315 to 325, Desirability increases sharply.

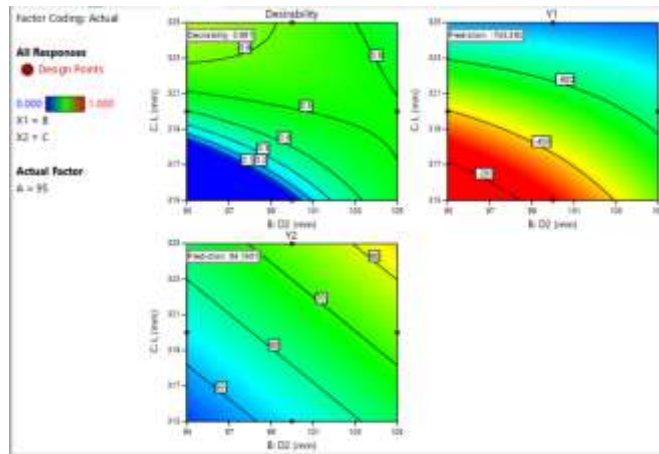


Figure 11: Contour plot of Desirability (A = 95)

Graph Figure 11 depicts the contour graph of Desirability when A (D1) is fixed at 95, showing the optimal values of B (D2) and C (L) to achieve the highest Desirability.

Desirability contour plot (A = 95):

- The highest Desirability is about 0.691 in region C about 321 and B about 97.

Y1 contour plot (A = 95):

- Mean Stress (Y1) is lowest in region C about 325 and B about 97 with a value of about -745.

Y2 contour plot (A = 95):

- Max Load (Y2) is lowest in region C about 315 and B about 95 with a value of about 50.

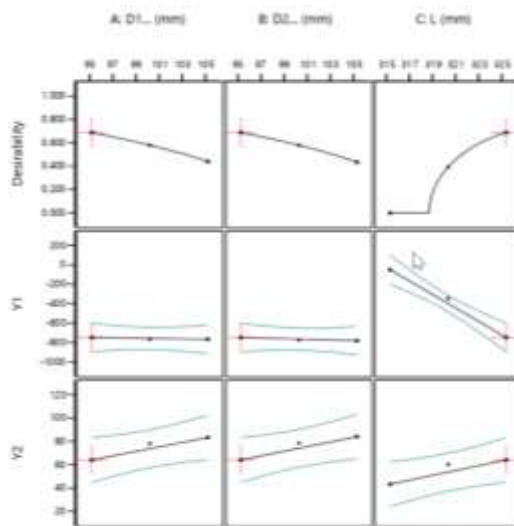


Figure 12. Contour plot of Y1 (Average Stress) and Y2 (Maximum Load) (A = 95)

Graph Figure 12 depicts the contour graph of Y1 (Mean Stress) and Y2 (Max Load) when A (D1) is fixed at 95, showing the optimal values of B (D2) and C (L) to achieve lowest Mean Stress and Max Load.

To optimize Desirability and achieve the smallest Y1 and Y2, combine the results from both graphs:

- A (D1) = 95 (remain the same as in the graph)
 - B (D2) \approx 97 (according to both Desirability and Y1 contour plot)
 - C (L) \approx 321 (according to Desirability contour plot)
- Optimal value:
- A (D1): 95 mm
 - B (D2): 97 mm
 - H (L): 321 mm

These values will help achieve the highest Desirability, while keeping Mean Stress (Y1) and Max Load (Y2) at the lowest possible level according to the analysis results.

Thus, to ensure optimal maximum stamping force and mean stress, the workpiece size should be selected as: {D1, D2, L}={95; 97; 321}mm



Figure13. The workpiece has been optimized

VI. CONCLUSION

In this article, the process of stamping turbine blade details was studied and the RSM method was used for optimization. To demonstrate the correctness and effectiveness of the proposed method, the stamping process is simulated, and the stamping results of the optimized blank and the conventionally designed blank are compared. The results show that:

- With this design, the mold cavity is guaranteed to be completely filled and the details are guaranteed. The shape

and edges are formed without hindering the detailed shaping process. The temperature of the part after stamping is still high, it is necessary to increase the shaping time or stamp several times to give the workpiece time to cool down.

- Organize the metal grain of the part without breaks or defects, ensuring technical requirements.
- Machines selected meet the required stamping force and capacity.
- It is necessary to regularly check to detect errors and defects in dangerous locations on the cavity of the mold
- Optimization results show that FEM combined with RSM can be used as a powerful tool to optimize complex forming processes such as turbine blade stamping process.

REFERENCES

- [1]. Y. K. Fuh et al., "Preform design with increased materials utilization and processing map analysis for aluminum hot forging process," *J. Manuf. Process.*, vol. 90, no. 300, pp. 14–27, 2023, doi: 10.1016/j.jmapro.2023.02.006.
- [2]. J. Yin, R. Hu, and X. Shu, "Closed-die forging process of copper alloy valve body: Finite element simulation and experiments," *J. Mater. Res. Technol.*, vol. 10, pp. 1339–1347, 2021, doi: 10.1016/j.jmrt.2020.12.087.
- [3]. X. Huang, Y. Zang, H. Ji, B. Wang, and H. Duan, "Combination gear hot forging process and microstructure optimization," *J. Mater. Res. Technol.*, vol. 19, pp. 1242–1259, 2022, doi: 10.1016/j.jmrt.2022.05.113.
- [4]. A. Alessio, D. Antonelli, R. Doglione, and G. Genta, "Die wear reduction by multifactorial Design of Experiments applied to forging simulations," *Procedia CIRP*, vol. 112, pp. 424–429, 2022, doi: 10.1016/j.procir.2022.09.031.
- [5]. F. Campi, M. Mandolini, C. Favi, E. Checcacci, and M. Germani, "An analytical cost estimation model for the design of axisymmetric components with open-die forging technology," *Int. J. Adv. Manuf. Technol.*, vol. 110, no. 7–8, pp. 1869–1892, 2020, doi: 10.1007/s00170-020-05948-w.
- [6]. Zhou, J., et al. (2013). Optimization of an aluminum alloy anti-collision side beam hot stamping process using a multi-objective genetic algorithm. *Archives of Civil and Mechanical Engineering*, 13(3), 401–411.
- [7]. Nguyen Van Canh, et al., "Application of CAD/CAM/CAE in modelling of Die for Hot Forging of Stainless Steel Valve," *International Journal of Scientific Engineering and Science*, Vol. 7, Issue 4, pp. 29-34, 2023.